



Research Article

Experimental investigation of the effect of longitudinal tensile reinforcement ratio on ductility behaviour in GPC beams

Ahmet ÖZBAYRAK^{*1}, Ali İhsan ÇELİK², Mehmet Cemal ACAR³, Ahmet ŞENER²

¹Department of Civil Engineering, Erciyes University Faculty of Engineering, Kayseri, Türkiye

²Department of Construction, Kayseri University, Tomarza Mustafa Akıncioğlu Vocational College, Kayseri, Türkiye

³Department of Construction, Kayseri University, Technical Science Vocational College, Kayseri, Türkiye

ARTICLE INFO

Article history

Received: 14 April 2024

Revised: 24 May 2024

Accepted: 04 June 2024

Key words:

Compressive and flexural strength, ductility, geopolymer concrete, reinforced concrete beam, strain limit

ABSTRACT

This research first determined the strength of the cylindrical geopolymer concrete materials under compressive stresses. Secondly, conventional and geopolymer-reinforced concrete beams were manufactured in different reinforcement ratios, and their mechanical properties were compared under bending. The main aim of this study is to experimentally compare the effect of reinforcement ratio on the ductility behavior of an alkali-activated geopolymer concrete (GPC) beam with that of an ordinary Portland cement (OPC) beam. First, balanced reinforcement calculations were made considering the mechanical properties obtained from the material tests. The load-displacement, moment-curvature, and crack development results obtained from beam tests are interpreted with this information. OPC and GPC beams exhibited similar strength and crack development behavior. However, the behavior of GPC and OPC concretes differs regarding the ductility index. Therefore, to achieve similar ductility in the conduct of GPC and OPC beams, the balanced reinforcement ratio and section dimensions of GPC beams should be chosen to be larger than OPC.

Cite this article as: Özbayrak, A., Çelik, A. İ., Acar, M. C., & Şener, A. (2024). Experimental investigation of the effect of longitudinal tensile reinforcement ratio on ductility behaviour in GPC beams. *J Sustain Const Mater Technol*, 9(2), 114–127.

1. INTRODUCTION

The production of Ordinary Portland Cement (OPC) harms the environment, which has sparked intense interest in creating new varieties of "green" geopolymer concrete. It is necessary to demonstrate the applicability of current design procedures or develop new design methodologies if geopolymer concretes are widely used in practice [1]. Davidovits invented geopolymer concrete (GPC) with superior properties in 1974 by using materials such as Silicon (Si) and Aluminium (Al) rich fly ash activated with alkaline liquids instead of Portland cement (OPC) as a binder in concrete [2–4]. Alkaline liquids are concentrated

aqueous alkali hydroxide or silicate solutions with soluble alkali metals, usually based on sodium (Na) or potassium (K). Highly alkaline liquids dissolve silicon and aluminum atoms in the source materials and form the geopolymeric binder. Efficiency in the production of geopolymer concrete is highly dependent on the types of aluminosilicate sources and activators [5, 6]. The raw material used as a source, alkaline solution concentrations, and curing conditions play an essential role in increasing the strength of geopolymer concrete by improving the polymerization process. The experimental results demonstrate that geopolymer concrete's mechanical qualities rise as the activator/binder ratio increases and the water/binder ratio decreases [7]. However,

*Corresponding author.

*E-mail address: ozbayrak@erciyes.edu.tr



the development of this material is still in its infancy. Further progress is needed to deal with the safety risk associated with the activating solution's high alkalinity and the polymerization reaction's hypersensitivity to temperature [8–10]. The advantages of geopolymer concrete are its high compressive and tensile strength, rapid strength gain, low shrinkage, and high temperature and chemical resistance [11–15]. Despite these advantages, the practical use of geopolymer concrete is quite limited. The main reason for its limited practical use is insufficient research on building elements, design, and application studies [16].

In the literature research, shear and bending behaviors of fly ash-based geopolymer-reinforced concrete beams were investigated structurally under chemical composition, reinforcement ratio, glass fiber content, and steel fiber use. The first studies on the structural behavior of fly ash-based geopolymer concrete beams were made by Sumajouw et al. [17]. They tested the bending behavior of six reinforced concrete beams with variable reinforcement ratios. As a result, it was determined that the flexural strength increased depending on the increase in the reinforcement ratio, as in the behavior of conventional reinforced concrete beams. In another study, sixteen reinforced concrete geopolymer beams with varying tensile reinforcement ratios (0.64–2.69%) and concrete compressive strength (37–76 MPa) were tested by M. Sumajouw and Rangan [18]. The effect of reinforcement ratio on geopolymer concrete beams in terms of bending capacity and ductility was similar to conventional reinforced concrete beams. In parallel studies, it has been reported that the flexural behavior of fly ash-based geopolymer concrete beams is identical to traditional reinforced concrete beams, such as initial cracking load, crack width, load-deflection relationship, bending stiffness, ultimate load, and failure mode [19–27]. The bending behaviors of geopolymer-reinforced and cementitious reinforced concrete beams were investigated by numerical analysis (ANSYS APDL) and confirmed by experimental studies. The deflection in the GPC beam was higher than in the OPC beam, and better crack propagation was found in the GPC beam than in the OPC beam. The applied specifications state that the GPC beam is a better alternative material for the beam [28]. It was determined by Jeyasehar et al. [29] that the initial crack load of geopolymer concrete beams was higher when compared to conventional cement-based concrete beams, but crack width, mid-span deflection, and final load were lower.

Another study for bending and deflection calculations evaluated the applicability of the ACI 318-2019 code for geopolymer concrete beams. It has been stated that a suitable model is needed to calculate the flexural strengths and deflections of geopolymer concrete beams after the first crack formation [30]. When adding glass fiber or steel fiber and hybrid propylene while manufacturing fly ash-based geopolymer-reinforced concrete beams, the bending capacity increased by 30–35% [31, 32]. Sathish Kumar et al. [33] experimentally tested the shear strength of geopolymer concrete beams by adding triple-blended hybrid fibers. Fracture beams were compared by adding steel and polypropylene fiber at different rates. As a result, combining hybrid fibers

improved the shear strength and changed the fracture type of the beams from shear to bending. However, the disadvantage of GPC beams is that they exhibit a more ductile behavior than OPC beams, and as a result, more small cracks occur in GPC beams compared to OPC beams [34].

On the other hand, the research conducted by Mourougane et al. [35] revealed that geopolymer concrete beams have higher shear strength in the range of 5–23% than conventional cement-based concrete beams. Based on research on a series of shear-critical geopolymer concrete beams with varying longitudinal and transverse reinforcement ratios, Chang concluded that the calculation method applied for conventional concrete beams could also be safely used to predict the shear strength of geopolymer concrete beams [36]. In the results of direct shear tests (shear aperture ratio) conducted by Visintin et al. [1], it was determined that the shear friction properties of the geopolymer concrete used in the experimental research behaved similarly in range to the shear friction properties of the commonly used OPC concrete.

This study compared the flexural behaviors of OPC (3 specimens) and GPC (3 specimens) beams with various reinforcement ratios, targeting an average strength of 30 MPa. To calculate the balanced reinforcement ratio, the compressive strength and mechanical properties of OPC and GPC concrete were determined by conducting preliminary material tests on cylindrical samples of $\varnothing 100 \times 200$ mm dimensions. This way, the stress-strain relationship and stress block design parameters of fly ash-based GPC and OPC were investigated for the balanced reinforcement ratio calculation. The equivalent pressure block height (a) at the moment of strain corresponding to the maximum stress of the cylindrical GPC specimens is approximately 30% higher than that of the OPC specimens [37]. Therefore, the balanced reinforcement ratio calculated for GPC concrete was larger. At the end of the experimental study, GPC beams were compared with OPC beams in load-displacement and moment-curvature relations. Similarities and differences were revealed regarding behavior and strength [38]. Although GPC beams exhibit similar properties to OPC beams in terms of maximum strength and crack development, increasing the beam section and reinforcement ratio is necessary for similar ductility in behavior.

1.1. Research Significance

In recent years, it has been revealed that geopolymer concrete (GPC) has superior properties compared to Portland cement concrete (OPC). However, more research is needed before GPC can be used in any area where OPC is used. With the increasing population and rapid urbanization, the demand for concrete is increasing exponentially. In addition, due to OPC production, 7–8% of CO_2 emissions are essential in improving the effect of greenhouse gases in the atmosphere. For these reasons, research on using fly ash material in the waste product class in concrete production is essential in making concrete more environmentally friendly. Previous studies have shown that the mechanical characteristics of geopolymer concrete, such as compressive strength and tensile strength, are superior to those of OPC concrete [39–45]. However, compared to

Table 1. Chemical components of fly ash

Components	%
SiO ₂ , x	59.2
Al ₂ O ₃ , y	20.3
Fe ₂ O ₃ , z	7.65
The sum of x, y, z	87.1
CaO	1.87
MgO	2.21
SO ₃	0.19
Na ₂ O	1.56
K ₂ O	2.36
Cl ⁻	0.05
LOI (loss of ignition)	3.23
Fineness (>45 μm)	17.4

typical cement-based concrete, geopolymer concrete has a lower elastic modulus [37, 41, 46–48]. Using geopolymer concrete as a structural element has no detrimental effect on load-bearing capacity, and the geopolymer concrete members could be safely designed following existing standards of practice [49]. However, more research is needed to accelerate the use of geopolymer concrete in large-scale field applications and provide more practical and cost-effective design guidelines for its use in structural members.

In the Research Significance section of the manuscript, the authors state the purpose of their study, which is to investigate the mechanical performance of GPC beams reinforced with steel bars. The survey results will assist in understanding the behavior of GPC beams and their load-carrying capacity and ductility. This information could potentially lead to the developing of more optimized and sustainable structural designs for buildings and infrastructures. Therefore, the study is significant as it advances construction materials and engineering knowledge.

2. MATERIALS AND METHODS

2.1. Materials

Low calcium fly ash (ASTM Class F) supplied from the İsken Sugözü Power Plant was used as the primary material in the production of geopolymer concrete. The chemical composition of the fly ash determined for this power plant based on XRF analysis is given in Table 1. Accordingly, the sum of x, y, and z being more than 70% indicates that the ash taken from the İsken Sugözü Power Plant meets the targeted strength and behavior requirements. Its specific gravity was 2.35 on average.

The research used a mixture of NaOH and Na₂SiO₃ solutions as an alkali activator. NaOH grains in the form of pallets used in sodium hydroxide solution are 98% pure. To prepare a 14 M sodium hydroxide solution, 560 grams of NaOH was added to 1 Liter of water. Before adding the NaOH solu-

tion to the concrete mix, it was kept at room temperature for 24 hours. The mixing ratios of the Na₂SiO₃ solution are Na₂O=13.5–15%, SiO₂=27–30%, H₂O=48–50% and the mass density is 1510 kg/m³. Crushed stone with a 7–11 mm diameter was used as coarse aggregate, and river sand was used as fine aggregate. To reduce the absorption of water and chemicals by the aggregate, the moisture content of the fine aggregate was kept as close to the saturated surface dry as possible.

2.2. Mixing Ratios

To reach the optimum ratio of various components of GPC concrete, preliminary studies have been conducted and published [50]. Accordingly, the parameters held constant in the current study include the aggregate content by weight (0.75), the ratio of fine aggregate to total aggregate (0.35), the proportion of alkali to fly ash by mass (0.60), and the ratio of Na₂SiO₃ to NaOH (1.5). The amount of material required to produce 1 m³ of GPC concrete according to the above ratios is given in Table 2 in kg.

While preparing the mixture, primarily coarse aggregate, fine aggregate, and fly ash were mixed for 3 minutes in a 125 dm³ concrete mixer. Afterward, the previously prepared Na₂SiO₃ and NaOH solutions were added to the mixture mortar one after the other for two more minutes. No water or plasticizer was added to the mixture during the total mixing period of 5 minutes. In the literature, it has been recommended that alkaline liquid be prepared by mixing sodium silicate and sodium hydroxide solutions and reacting thoroughly for at least 24 hours before use [22]. However, such an application was not made in the study since it was determined to accelerate the setting time. Furthermore, since 14 M sodium hydroxide causes the presence of excess NaOH ions, it leads to rapid and early precipitation of the aluminosilicate gel, leading to rapid hardening and inhibiting the formation of other geopolymeric precursors [51].

2.3 Experiment Samples

GPC and OPC beams with dimensions of 150 mm width, 200 mm depth, and 1100 mm span length were produced, targeting a compressive strength of 30 MPa as the intended strength and varying tensile reinforcement ratios. Tensile reinforcement ratios were determined as the lower limit (0.003), the upper limit (0.02), and a value between both specified in the ACI 318 specification [52, 53]. 2Ø8 longitudinal reinforcement was used in the compression region of all samples produced. The transverse reinforcement (stirrup) is adjusted to be 8Ø8/150 mm in each beam. The research tested six beams using three different GPC and OPC beams that matched each other. The transverse reinforcements were sized so that the concrete cover was 25 mm. The cross-section and reinforcement information of the beams are given in Table 3, and the longitudinal and transverse reinforcements are placed in Figure 1.

Table 2. GPC mixing ratios (kg/m³)

Class F fly ash	Sodium silicate solution	Sodium hydroxide solution	Extra added water	Plasticizer	Fine aggregate	Coarse aggregate
406	146	97	–	–	643	1194

Table 3. Beam geometry and reinforcement information

Group	Sample name	Reinforcements		Tensile reinforcement ratio	Curing	ρ_{min}	ρ_b	0.85xpb
		Compression reinforcement	Tensile reinforcement					
1	OPC1	2Ø8	2Ø8	0.003	28 days	0.0028	0.025	0.021
	OPC2	2Ø8	3Ø14	0.017	28 days			
	OPC3	2Ø8	2Ø18	0.019	28 days			
2	GPC1	2Ø8	2Ø8	0.003	24h 90 °C	0.0028	0.025	0.021
	GPC2	2Ø8	3Ø14	0.017	24h 90 °C			
	GPC3	2Ø8	2Ø18	0.019	24h 90 °C			

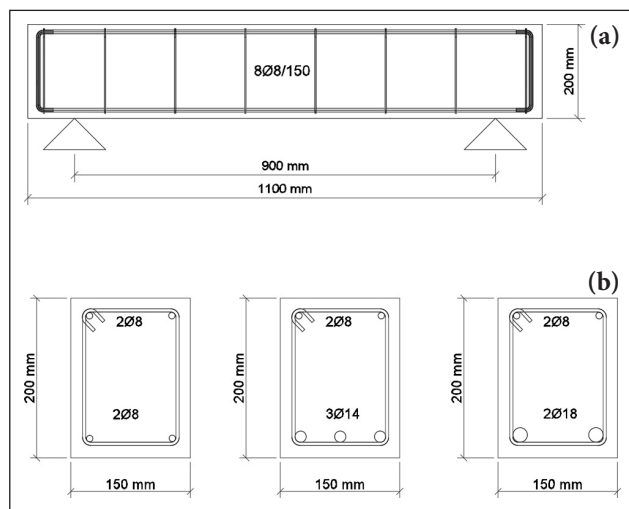


Figure 1. (a) Beam longitudinal section and transverse reinforcements, (b) Beam cross-sections and longitudinal reinforcements.

Table 4. Reinforcement properties under axial tension

Rebar diameter (mm)	f_y (MPa)	f_u (MPa)	ϵ_p (%)	f_u / f_y
Ø8	424	541	37.5	1.27
Ø14	453	572	32.8	1.26
Ø18	456	564	24.4	1.24

f_y : Yield strength; f_u : Tensile strength; ϵ_p : Unit elongation at break.

In the experimental study, B420c reinforcement was used following the standards, and the tensile strength/yield strength ratio was determined to be between 1.15 and 1.35. The ratio of yield strength, tensile strength, unit elongation at break, and tensile strength to yield strength of the longitudinal and transverse reinforcements used in the research are in Table 4.

2.4. Casting and Curing

Geopolymer-reinforced concrete beams were poured into plywood molds with dimensions of 150x200x1100 mm in the laboratory. A bottle-type vibrator was used to compact the concrete. The average slump value was determined as 21 cm in the measurements made during casting. Curing was done in a laboratory oven at 90 °C for 24 hours without mold removal. The research recommended curing after a rest period of 0–5 days after casting. To obtain the best results regarding compressive strength, geopolymer samples were kept for four days before curing [54]. Traditional reinforced concrete beams were produced in a ready-mixed concrete plant. The concrete is placed in the prepared beam molds, and the curing stages are shown in Figure 2.

2.5. Experiment Setup and Loading Procedure

The precise span length of tested beams is 900 mm and simply supported, fixed at one end, and sliding joint at the other. The load was applied to the beam by a 300 kN servo-hydraulic actuator from a single loading point in the middle of the span (Fig. 3). The ratio obtained by dividing



Figure 2. Placing and curing concrete in molds.

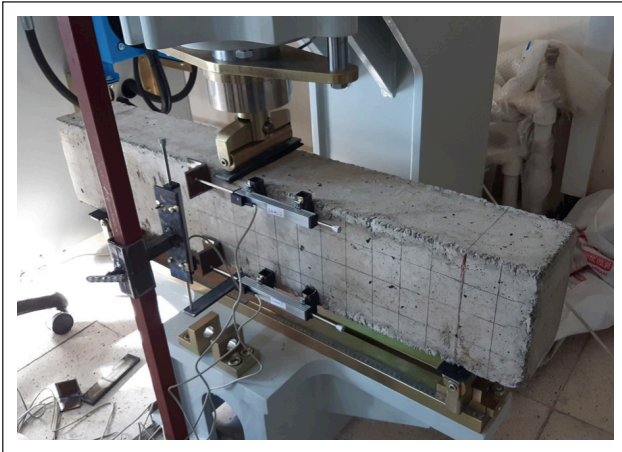


Figure 3. Experiment setup and measuring instruments.

the shear span ($a=0.9/2=0.45$) by the average adequate depth ($d=0.175$) is found to be $a/d=0.257$ (considering the variation in sufficient depth, ± 0.04). The beam's cross-sectional height (0.2 m) is not greater than 1/4 of its clear span ($0.9/4=0.225$ m), so it is classified as a standard beam. To prevent local crushing of the concrete, hard rubber, and leather belts are placed between the steel rollers and the concrete surface in the loading and bearing areas. The load was applied by controlling the displacement of the actuator at a rate of 2 mm/s until 50 mm of deflection occurred. Next, two LVDTs (Linear Variable Data Transformers) were placed on the middle span upper and lower beam faces to determine the moment-curvature relationship by measuring the shortening in the upper fibers of the beam and the elongation in the lower fibers. Again, a third LVDT was added to the experimental setup to determine the load-deflection relationship by taking vertical measurements from the beam middle span. The measurements taken during the experiment were transferred to the computer with the help of a data logger.

3. RESULTS

3.1 Material Tests

Material tests are essential in the interpretation of beam behavior and strength. For this reason, three $\varnothing 100 \times 200$ mm cylindrical specimens were prepared for each group, and unit strain, modulus of elasticity, Poisson's ratio, and compressive strength were calculated [37, 55]. The weight, unit volume weight, and slump values measured from the average of the samples in each group before the tests are given in Table 5. It has been determined that GPC and OPC are similar in unit volume weight.

The characteristic strength properties, corresponding to the targeted 30 MPa and the obtained strengths, are provided in Table 6 by averaging the concrete samples in each group. The ratio of transverse strain to longitudinal strain (Poisson), modulus of elasticity, and ductility due to deformation were obtained differently in GPC and OPC samples. In the calculation of the elastic modulus, firstly, 40% of the maximum stress (f_{ck}) is taken, and the elastic stress limit (f_d) is determined (Fig. 4).

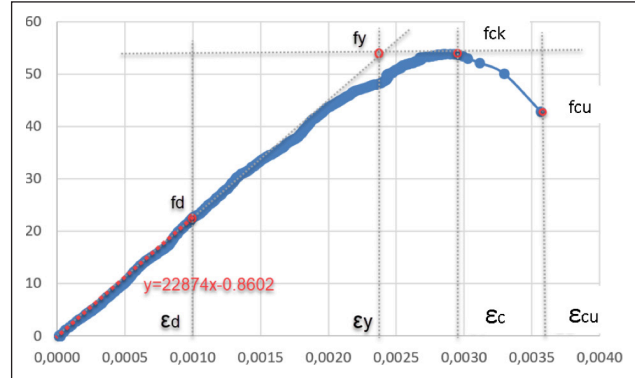


Figure 4. Example calculation of elastic modulus and ductility from the concrete stress-strain curve.

Table 5. Average slump and unit volume mass

Group name	Slump cm	Weight kg	Unit volume mass kg/m^3
OPC	16	3.662	2330
GPC	21	3.739	2380

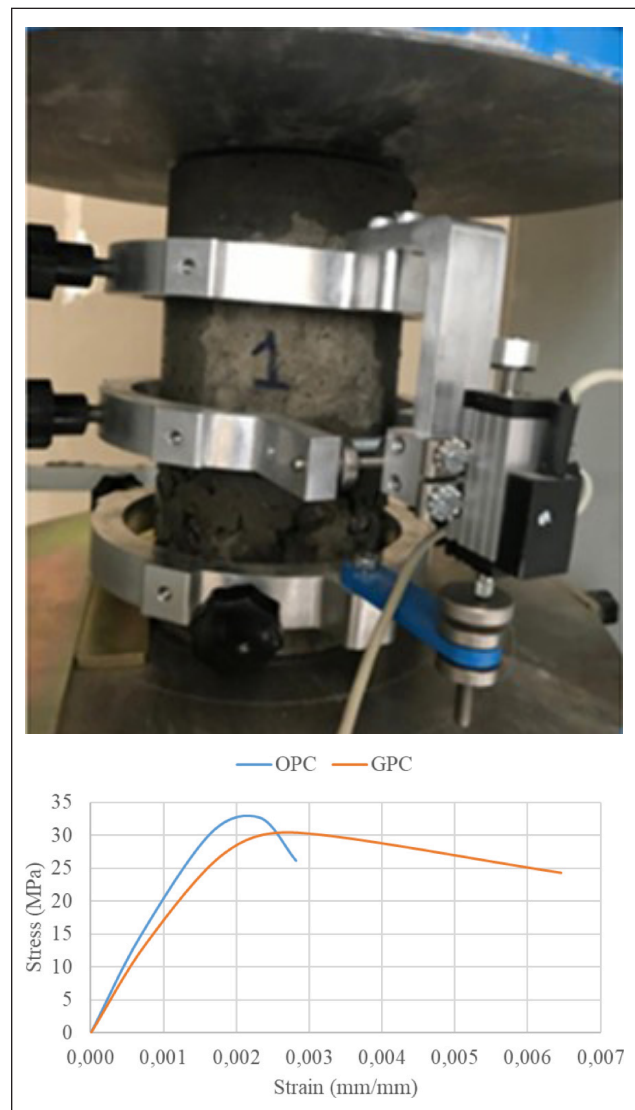


Figure 5. Stress-strain curves.

Table 6. Characteristic strength properties of materials (MPa - mm/mm)

Group name	E_c	f_d	f_y	f_{ck}	f_{cu}	v_c
OPC	19128	14.71	30.34	32.70	26.16	0.20
GPC	16913	13.69	27.40	30.43	24.34	0.30
Group name	E_s	ϵ_d	ϵ_y	ϵ_c	ϵ_{cu}	$\mu = \epsilon_{cu} / \epsilon_y$
OPC	210000	0.00068	0.00165	0.00232	0.00282	1.71
GPC	210000	0.00077	0.00185	0.00284	0.00646	3.50

E_c : Concrete modulus of elasticity; E_s : Steel modulus of elasticity; v_c : Poisson's ratio; f_d : Concrete elastic stress; f_y : Concrete yield stress; f_{ck} : Concrete maximum stress; f_{cu} : Concrete ultimate stress; ϵ_d : Concrete strain corresponding to elastic stress; ϵ_y : Concrete yield strain; ϵ_c : Concrete strain corresponding to maximum stress; ϵ_{cu} : Concrete strain corresponding to ultimate stress; μ : Material ductility (compression ductility).

Table 7. Balanced reinforcement ratios (N-mm)

Group name	ϵ_s	ϵ_{cu}	$\epsilon_{cu} E_s$	k_1	d	x	a	f_{cd}	ρ_b
OPC	0.0018	0.00282	592.20	0.821	175	105.70	86.79	21.8	0.0258
GPC	0.0008	0.00646	1357.3	0.837	175	135.96	113.8	20.3	0.0312

Then, a trend line (red line) was added to f_d from the starting point (0, 0) of the stress-strain graph, and the equation of this line was displayed. The modulus of elasticity was calculated by finding the expression y/x in this equation. Ductility is the ratio of ultimate strain (ϵ_u) to yield strain (ϵ_y). ϵ_{cu} is the strain of the ultimate stress (f_{cu}), corresponding to approximately 85% of the f_{co} . ϵ_y is the strain corresponding to the yield stress (f_y). f_y is the intersection point of the trend line for which the elastic modulus is calculated, and the line that passes horizontally through the axis corresponds to f_{ck} (gray lines). In the equation $y=22874x-0.8602$, the value of $x=\epsilon_y$ is obtained by substituting the value of f_{ck} for y . Thus, the ductility value was calculated from the experimental data of the stress-strain curve using the formula $\mu=\epsilon_u/\epsilon_y$.

A comparison of the average stress-strain curves of GPC and OPC concrete samples is given in Figure 5. The strain corresponding to the maximum stress of GPC is more significant than that of OPC.

3.2. Balanced Reinforcement Ratio

Only a few studies on the stress-block parameters for fly-ash-based GPC under heated curing conditions have been reported in the literature, even though there have been many studies on the rectangular stress-block parameters for conventional Portland concrete [56, 57]. Nevertheless, the research findings demonstrate that it is still appropriate and highly accurate to design GPC beams using the ACI standards for concrete structures [58].

In the cylinder compression tests, the maximum deformations (ϵ_{cu}) of GPC and OPC concretes at ultimate load are different (Table 6). This table shows that according to GPC (0.00646), the balanced reinforcement ratio calculation will differ from OPC (0.00282), depending on the ultimate strain corresponding to the concrete crushing change. It is important to make balanced reinforcement calculations to prevent brittle fractures in beams. Equation 1 represents the calculation of x , the depth of the compressive stress block based on the strain values of steel and concrete at yield and crushing. Equation 2 represents the calculation

of the balanced reinforcement ratio (ρ_b) using the strain values of concrete at crushing obtained from cylinder pressure tests. The main reason for the different balanced reinforcement ratios is that the crushing strain values of GPC and OPC concrete differ, resulting in different values of ρ_b .

$$\frac{d}{x} = \frac{\epsilon_{sy} + \epsilon_{cu}}{\epsilon_{cu}} \times \frac{E_s}{E_c} \quad \text{and} \quad x = \frac{a}{k_1} \quad (1)$$

$$\rho_b = \frac{A_{sb}}{bd} = 0.85k_1 \frac{f_{cd}}{f_{yd}} \times \frac{\epsilon_{cu}E_s}{\epsilon_{cu}E_s + f_{yd}} \quad (2)$$

The coefficient k_1 , the ratio between the average and maximum stress, was calculated in Eq. 3 according to ACI 318 for the characteristic cylindrical compressive strength $f_{ck} > 28$ MPa.

$$k_1 = (1.05 - 0.007f_{ck}) \geq 0.65 \quad (3)$$

The calculated balanced reinforcement ratio values are given in Table 7. Accordingly, it is seen that the tensile reinforcement ratios ($\rho < \rho_b$) of all beam samples shown in Table 3 are below the balanced reinforcement ratio. In this case, tensile failure is expected to occur in all beams.

The equivalent compressive block height (a) of the GPC samples at the moment of maximum stress is greater than that of the OPC samples. However, Figure 6 shows that the GPC samples achieve their ultimate load capacity at lower deflection values than the OPC samples (Fig. 6a). Using more tensile reinforcement in GPC beams is necessary to achieve similar ductility with OPC beams. For this reason, the balanced reinforcement ratio of GPC beams is higher than that of OPC beams. However, this inference is applicable for fracture scenarios due to bending. In cases of fracture due to shear, the situation is different. Table 7 shows that the reinforcement in GPC does not yield at the point of concrete crushing. Additionally, the strain of GPC concrete at the end of crushing is greater than that of OPC concrete

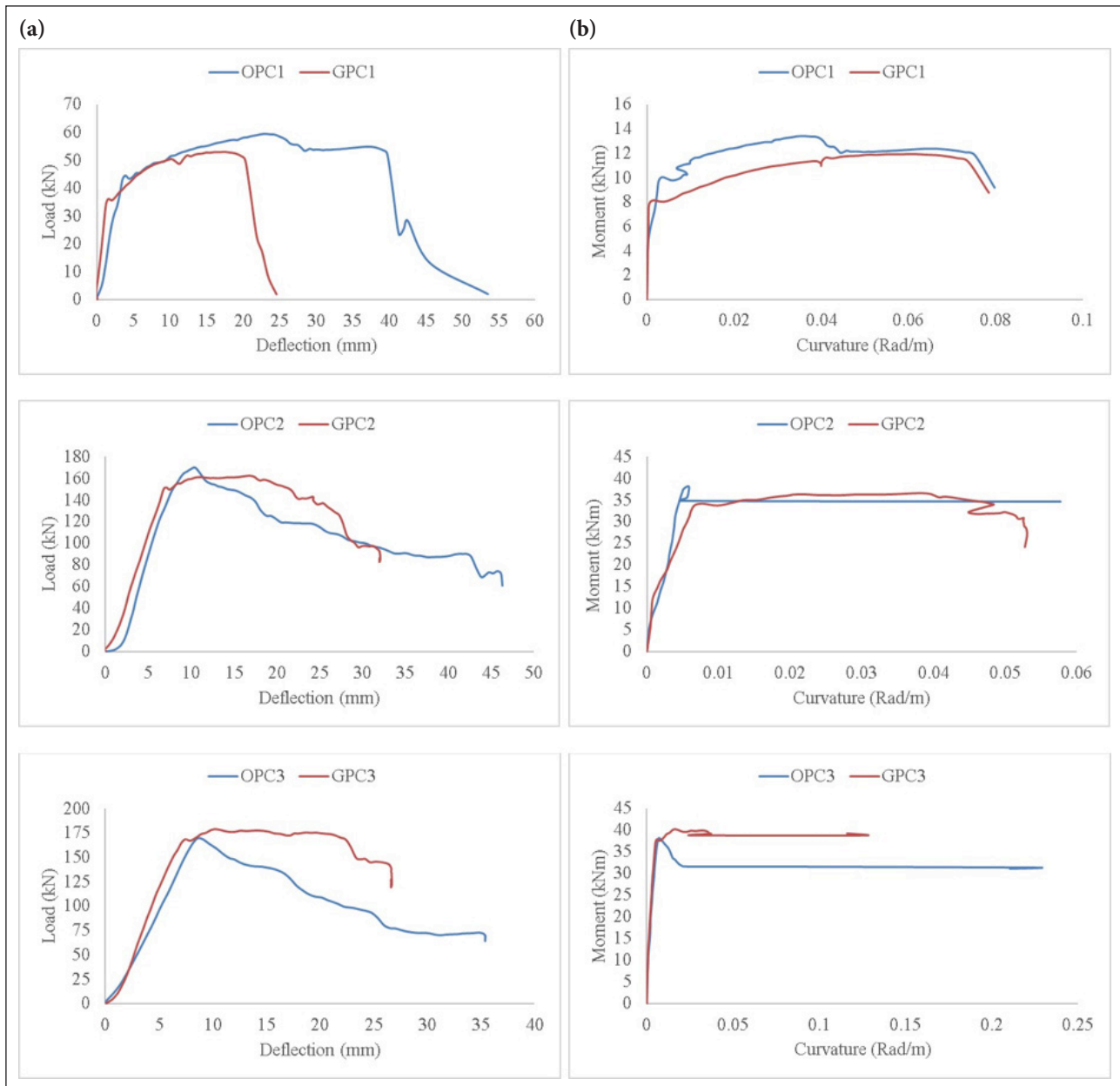


Figure 6. (a) Load displacement curves, (b) Moment curvature relationship.

due to its slightly lower modulus of elasticity, indicating that GPC is weaker regarding shear. It has been determined that the reinforcement in OPC concrete beams reaches the total yield strain at the ultimate load capacity.

3.3. Beam Tests

The load-displacement and moment-curvature graphs of the beam samples with different reinforcement ratios are as given in Figure 6.

For values of a concrete compressive strength less than 50MPa, the maximum reinforcement ratio defined in ACI 318 is 0.02 [52, 53]. This condition must be met for a tensile fracture to occur under the influence of ductile behavior. Therefore, the deformation capacity of GPC beams is lower than OPC beams, and the need for tensile reinforcement is higher. However, the balanced reinforcement ratio calculated for GPC ($\rho_b=0.031$) exceeds the limit value ($\rho=0.02$)

given in ACI 318 for OPC. In this case, GPC beam section dimensions should be more significant than OPC beam section dimensions to provide sufficient ductility.

The strains corresponding to compressive stresses in geopolymer concrete are higher than in conventional concrete. For this reason, geopolymer concrete's material ductility (compression ductility) was greater than conventional concrete's (Table 6). In the first experiments, where the reinforcement ratio is low (0.003), the GPC1 beam has a deflection capacity of less than the OPC1 beam (Fig. 6a). The OPC concrete in the compression zone reached its fracture strength after the reinforcement in the tensile zone yields. Concrete crushing in the compression zone in GPC can reach similar strength due to considerably larger than in OPC. As a result, the yielding of tensile reinforcement is the determining factor in GPC beams, which produce a

Table 8. Moment values for reinforcement yielding (M_y)

kNm	OPC1	GPC1	OPC2	GPC2	OPC3	GPC3
Experimental M_y	10.0	8.12	37.9	34.1	37.6	37.1
Analytical M_y	7.10	–	29.2	–	32.0	–

later compressive strength response than OPC beams. As a result, the beam collapses from oblique tensile failure before reaching the maximum compression fracture. In experiments second and third, the increase in reinforcement ratios increased the load-carrying capacity of the beams and became a determinant of flexural stiffness. However, the shear tension failure occurred (Fig. 6a).

Due to the high ductility of the material, GPC beams show lower stiffness in the compression region and reach the moment-carrying capacity earlier than OPC beams for similar curvature values. The curvature values of the GPC and OPC beams were found to be close to each other since the failure of the first beams occurred due to the reinforcement yielding in the tension zone (Fig. 6b). However, the tension reinforcement ratio increased in the second and third beams. Due to the high ductility value in GPC, the compressive stresses formed in the upper beam fiber remained at lower levels for curvature values similar to those of OPC. This high ductility reduced the strength contribution of the concrete in the compression zone during bending. As a result, the load in GPC beams is carried mainly by the tension reinforcement. In the second and third experiments, the beams reached the bearing capacity at higher curvature values than the OPC beams (Fig. 6b).

Oblique tensile and shear compression fractures occurred in beam samples due to shear and flexural cracks ($a/d=2.57$). In the GPC1 and OPC1 samples, flexural tensile fracture occurred due to the rupture of the reinforcement by yielding. In the other beam samples (GPC2-OPC2 and GPC3-OPC3), only shear cracking occurred without bending cracks, resulting in sudden power depletions (Fig. 7). The inclined crack formed in the body in the first stage progressed rapidly and caused brittle fractures. As a result, shear compression collapses occurred in the beams without yielding the tensile reinforcements. However, the bearing capacity moment values increased due to increased reinforcement ratios (Table 8).

When the tests are examined in terms of load-displacement relations in Figure 6, it is seen that only in the first experiments is a load below the shear capacity applied to the beams. The way the beams break is a flexural tensile failure, which confirms this situation. In the second and third experiments, shear pressure fracture occurred due to the load applied to the beams above the shear strength (Fig. 7). The maximum analytical shear loads that OPC beams with the properties specified in the research can carry were calculated as 162 kN.

4. DISCUSSION

As a result of the material and beam tests, it was determined that geopolymer concrete (GPC) has a similar strength to conventional concrete but exhibits different behavior characteristics. Specifically, the increase in mate-

rial ductility (compression ductility) according to cylinder pressure tests caused a decrease in section ductility in beam bending tests. While the energy consumption capacity of GPC was higher in compressive strength tests, conventional concrete (OPC) performed better in energy consumption in beam tests focused on flexural strength.

Since the modulus of elasticity of GPC is lower and the strain corresponding to the maximum compressive stress is more significant than that of OPC concrete, the flexural stiffness is lower than that of OPC. This condition shows that the GPC-reinforced concrete beam will deflect more under the effect of bending. The calculations in the previous sections demonstrated the necessity of increasing the tensile reinforcement to exhibit similar stiffness to the OPC beam. In addition, increasing the flexural reinforcement alone may not be sufficient for the required stiffness not to exceed the reinforcement upper limit (0.02) set by regulations such as ACI318 and TS500. In this case, it may be necessary to increase the section dimensions for sufficient flexural stiffness. However, the experiments were terminated due to shear damage, especially in the last two experiments. This does not affect the flexural findings based on the material tests. Future studies should support these findings by conducting studies in which flexural fractures of beams can be observed.

4.1. Parameters Considered for OPC and GPC

4.1.1. Material Tests

- **Compressive Strength:** The compressive strength of GPC, determined through material tests, was comparable to that of OPC.
- **Elastic Modulus:** The elastic modulus of GPC was lower than that of OPC, as indicated by the values obtained from cylindrical samples [59–64].
- **Poisson's Ratio:** The Poisson's ratio of GPC was higher than that of OPC [65–68].
- **Strain at Maximum Stress:** The strain value corresponding to the maximum stress of GPC was higher than that of OPC [69, 70]. This difference increased as it approached the ultimate strain.
- **Ductility:** The increased yield and ultimate state strain values of GPC improved its ductility [71, 72]. Consequently, the equivalent pressure block height of GPC was greater than that of OPC, indicating that GPC beams would reach their bearing capacity at lower deflection values. Therefore, more tensile reinforcement is required to achieve similar ductility with OPC beams, resulting in a higher balanced reinforcement ratio for GPC.

4.1.2. Beam Tests

- **Reinforcement Ratios:** Three different reinforcement ratios were used in beam experiments. Beams in the first group failed due to flexural tensile fractures follow-

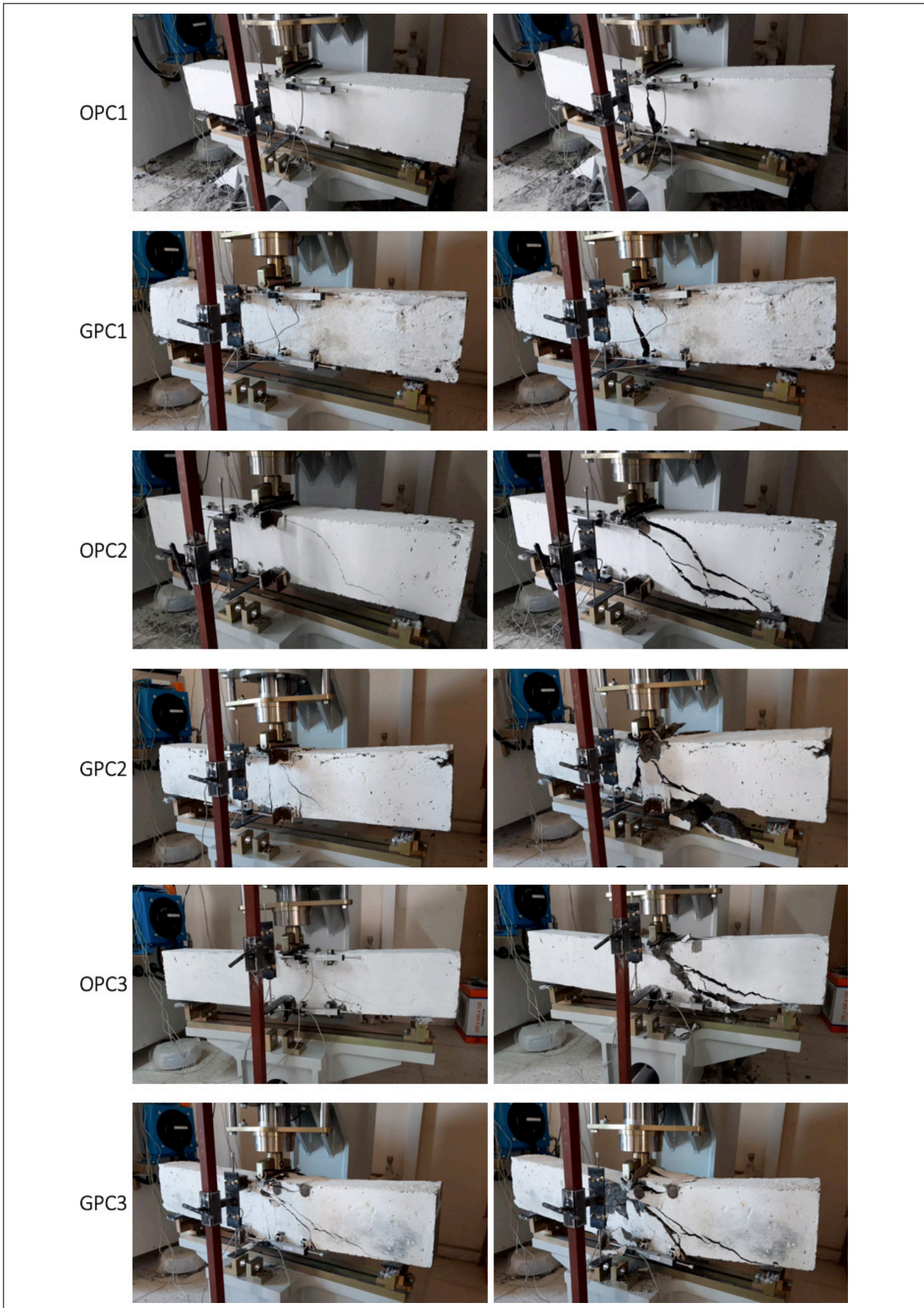


Figure 7. Crack development (left image: during the experiment, right image: at the end of the experiment).

ing reinforcement yield. In the last two groups, failure occurred due to shear pressure fractures in the beams without reinforcement yielding.

- Deflection Values: GPC beams reached maximum bearing capacity at lower deflection values than OPC beams [73, 74]. This indicates that the section ductility of GPC beams is lower despite higher material ductility [20, 75].
- Energy Consumption: The decrease in section ductility negatively affected energy consumption. In the first experiment, moment-curvature graphs were similar because the concrete was crushed when the reinforcement yielded. However, the graphs differed in the last two tests as the concrete collapsed according to the shear and compressive strength before reinforcement yield. The demand for compressive strength due to high deformation from GPC material tests led to decreased section ductility by consuming energy before OPC.

4.2. Advantages and Weaknesses of GPC over OPC

4.2.1. Advantages

- Higher Ductility: GPC exhibits higher material ductility, enhancing its energy consumption capacity in compressive strength tests.
- Environmental Benefits: GPC production is typically more environmentally friendly, as it can utilize industrial waste products such as fly ash and slag [76–78].

4.2.2. Weaknesses

- Lower Elastic Modulus: GPC's lower elastic modulus leads to higher deflections under load, reducing its flexural stiffness compared to OPC.
- Section Ductility: GPC beams have lower section ductility, negatively impacting their performance in flexural applications. The high material ductility of GPC, observed in cylinder tests, delays the compressive strength response in flexural tests, causing earlier energy depletion in shear and tensile effects.
- Design Adjustments: To achieve similar stiffness and ductility to OPC beams, GPC beams require more tensile reinforcement and potentially larger cross-sectional dimensions.

4.3. Recommendations for Beam Design and Standards

Given the experimental findings, it is crucial to consider the implications of these differences in practical applications:

4.3.1. Reinforcement Ratio and Standards Compliance

- The balanced reinforcement ratio limit should be strictly adhered to per standards such as ACI 318. The experiments indicated a higher balanced reinforcement ratio for GPC, suggesting a need for careful design adjustments.
- The designs used in the experiments might not fully comply with ACI standards due to the higher reinforcement ratios. Future designs should aim for compliance to ensure valid comparisons and safe structural performance.

4.3.2. Cross-Sectional Dimensions

- The conclusion that beam dimensions should be increased for GPC is based on the need for sufficient

flexural stiffness. While this approach may address the immediate stiffness issues, it is important to consider it within the framework of standard design practices.

- The suggestion to enlarge cross-sectional dimensions must be carefully evaluated, particularly when the beam is completely bending. If the reinforcement ratio in the beam is lower than the balanced reinforcement ratio, the behavior of the beam could differ significantly.

4.3.3. Future Research Directions

- The current findings are valuable and highlight key differences between GPC and OPC. However, definitive statements should be avoided until further studies, particularly those observing flexural failures in beams, are conducted.
- Future research should focus on verifying these findings with larger sample sizes and varied loading conditions to develop a more comprehensive understanding of GPC's behavior under different structural demands. By incorporating these considerations and adhering to established standards, the structural applications of GPC can be optimized to leverage its advantages while mitigating its weaknesses.

5. CONCLUSIONS

The high ductility of the material in geopolymer concretes causes a delay in the response of the compressive strength due to deflection. The increase in curvature causes a collapse in the form of tension and shear. The delayed pressure response on the beam's neutral axis causes the beam's energy to be depleted in shear and tensile effects before reaching the maximum compressive strength. All the obtained findings related to strength and deformation support each other. In general, GPC and OPC concrete exhibit similar behavior in terms of tensile and shear strengths. Still, the delayed compressive strength demand due to the ductility of GPC concrete reduces its section ductility and energy absorption capacity. For these reasons, it was determined that the balanced reinforcement ratio in GPC beams should be increased. In this case, larger sizes of GPC beams should be produced compared to OPC beams to have similar bending strength and energy consumption properties to prevent brittle fractures and maintain the upper limit of the reinforcement of 0.02. As a result, GPC concrete with low modulus of elasticity and high strain properties achieves similar stress values to OPC concrete ($\sigma = E \cdot \epsilon$). Although there is no significant difference in strength, they differ in deflection.

- High Ductility and Delayed Response: The high material ductility of geopolymer concrete (GPC) causes a delay in the compressive strength response due to deflection. This delay and increased curvature lead to tension and shear collapses.
- Energy Depletion in Shear and Tensile Effects: The delayed pressure response on the beam's neutral axis causes the beam's energy to be depleted in shear and tensile effects before reaching maximum compressive strength.
- Consistency of Findings: All findings related to strength

and deformation support each other. GPC and OPC concrete exhibit similar behavior in terms of tensile and shear strengths.

- **Reduced Section Ductility:** Due to the material ductility of GPC concrete, the delayed compressive strength demand reduces its section ductility and energy absorption capacity.
- **Balanced Reinforcement Ratio:** The balanced reinforcement ratio in GPC beams should be increased to achieve bending strength and energy consumption properties similar to those of OPC beams.
- **Larger Beam Sizes:** Larger GPC beams should be produced compared to OPC beams to achieve similar bending strength and energy consumption properties. This necessity arises because the modulus of elasticity of GPC is lower, and the strain corresponding to the maximum compressive stress is more significant than that of OPC concrete. Consequently, the flexural stiffness is lower, leading to more deflection under bending.
- **Stress and Strain Relationship:** GPC concrete with a low modulus of elasticity and high strain properties achieves similar stress values to OPC concrete ($\sigma = E \cdot \epsilon$). However, they differ in deflection despite similar strength.
- **Flexural Reinforcement and Section Dimensions:** Increasing the tensile reinforcement in GPC beams is necessary to exhibit similar stiffness as OPC beams. However, merely increasing flexural reinforcement may not suffice for the required stiffness due to regulatory limits. Therefore, increasing section dimensions may be needed for adequate flexural stiffness. This consideration is based on calculations and is consistent with the results of the material tests, even though some experiments were terminated due to shear damage.
- **Comparative Behaviour:** Geopolymer concrete unit weight, maximum compressive and flexural strengths, crack development, and fracture patterns are similar to conventional reinforced concrete structures. Deflection and ductility values differ between GPC and OPC. GPC beams require a higher balanced reinforcement ratio or larger section dimensions to achieve ductility, similar to OPC beams.
- **Recommendations for Future Studies:** Further studies should be conducted better to understand the behavior of geopolymer structural carrier system elements. This will help optimize the use of GPC in structural applications and ensure compliance with design standards. Additionally, future studies should focus on flexural fractures of beams to support and expand on the current findings.

As a result, geopolymer concrete unit weight, maximum compressive and flexural strengths, crack development, and fracture patterns are similar to conventional reinforced concrete structures. However, the deflection and ductility values are different in terms of behavior. Therefore, to achieve similar ductility in the behavior of GPC and OPC beams, the balanced reinforcement ratio or section dimensions of GPC beams should be chosen to be larger than OPC. Further studies on the subject should be increased better to understand the behavior of geopolymer structural carrier system elements.

ACKNOWLEDGMENTS

We want to thank Kayseri Beton firm and Önder Işık and Hasan Şahbaz for their contribution to the project.

ETHICS

There are no ethical issues with the publication of this manuscript.

DATA AVAILABILITY STATEMENT

The authors confirm that the data that supports the findings of this study are available within the article. Raw data that support the finding of this study are available from the corresponding author, upon reasonable request.

CONFLICT OF INTEREST

The authors declare that they have no conflict of interest.

FINANCIAL DISCLOSURE

This research was financially supported by the Kayseri University Projects Unit (BAP-FKB-2020-1013).

USE OF AI FOR WRITING ASSISTANCE

Not declared.

PEER-REVIEW

Externally peer-reviewed.

REFERENCES

- [1] Visintin, P., Mohamed Ali, M. S., Albitar, M., & Lucas, W. (2017). Shear behavior of geopolymer concrete beams without stirrups. *Constr Build Mater*, 148, 10–21. [\[CrossRef\]](#)
- [2] Lloyd, N., & Rangan, B. (2010). Geopolymer concrete: A review of development and opportunities. In *35th Conference on Our World in Concrete and Structures*, pp. 25–27.
- [3] Kotwal, A. R., Kim, Y. J., Hu, J., & Sriraman, V. (2015). Characterization and early age physical properties of ambient cured geopolymer mortar based on Class C fly ash. *Int J Concr Struct Mater*, 9(1), 35–43. [\[CrossRef\]](#)
- [4] Luhar, S., Chaudhary, S., & Luhar, I. (2019). Development of rubberized geopolymer concrete: Strength and durability studies. *Constr Build Mater*, 204, 740–753. [\[CrossRef\]](#)
- [5] Madheswaran, C. K., Ambily, P. S., Dattatreya, J. K., & Ramesh, G. (2015). Experimental studies on behaviour of reinforced geopolymer concrete beams subjected to monotonic static loading. *J Inst Eng India Ser A*, 96(2), 139–149. [\[CrossRef\]](#)
- [6] Duxson, P., Fernández-Jiménez, A., Provis, J. L., Lukey, G. C., Palomo, A., & Van Deventer, J. S. J. (2007). Geopolymer technology: The current state of the art. *J Mater Sci*, 42(9), 2917–2933. [\[CrossRef\]](#)
- [7] Pham, D. Q., Nguyen, T. N., Le, S. T., Pham, T. T., & Ngo, T. D. (2021). The structural behaviours of steel reinforced geopolymer concrete beams: An experimental and numerical investigation. *Structures*, 33, 567–580. [\[CrossRef\]](#)

- [8] Tyson, S., & Tayabji, S. (2010). Geopolymer Concrete (No. FHWA-HIF-10-014). United States. Federal Highway Administration.
- [9] Al Bakri, A. M., Kamarudin, H., Bnhussain, M., Nizar, I. K., Rafiza, A. R., & Zarina, Y. (2012). The processing, characterization, and properties of fly ash based geopolymer concrete. *Rev Adv Mater Sci*, 30(1), 90–97.
- [10] Ryu, G. S., Lee, Y. B., Koh, K. T., & Chung, Y. S. (2013). The mechanical properties of fly ash-based geopolymer concrete with alkaline activators. *Constr Build Mater*, 47, 409–418. [CrossRef]
- [11] Fernandez-Jimenez, A., Palomo, A., & Lopez-Hombrados, C. (2006). Engineering properties of alkali-activated fly ash concrete. *ACI Mater J*, 103(2), 106. [CrossRef]
- [12] Hardjito, D., Wallah, S., Sumajouw, D., & Rangan, B. (2004). On the development of fly ash-based geopolymer concrete. *Mater J*, 101(6), 467–472. [CrossRef]
- [13] Hardjito, D., Wallah, S., Sumajouw, D., & Rangan, B. (2004). Properties of geopolymer concrete with fly ash as source material: Effect of mixture composition. *Spec Publ*, 222, 109–118.
- [14] Delair, S., Prud'homme, É., Peyratout, C., Smith, A., Michaud, P., Eloy, L., Joussein, E., & Rossignol, S. (2012). Durability of inorganic foam in solution: The role of alkali elements in the geopolymer network. *Corros Sci*, 59, 213–221. [CrossRef]
- [15] Cheng, T. W., & Chiu, J. P. (2003). Fire-resistant geopolymer produced by granulated blast furnace slag. *Miner Eng*, 16(3), 205–210. [CrossRef]
- [16] Ma, C. K., Awang, A. Z., & Omar, W. (2018). Structural and material performance of geopolymer concrete: A review. *Constr Build Mater*, 186, 90–102. [CrossRef]
- [17] Sumajouw, D. M. J., Hardjito, D., Wallah, S. E., & Rangan, B. V. (2005). Behaviour and strength of reinforced fly ash-based geopolymer concrete beams. *Australian Structural Engineering Conference 2005*, pp. 453.
- [18] Sumajouw, M. D. J., & Rangan, B. V. R. (2006). Low-calcium fly ash-based geopolymer concrete: Reinforced beams and columns. *Curtin Univ Technol*. https://espace.curtin.edu.au/bitstream/handle/20.500.11937/23928/19466_downloaded_stream_558.pdf
- [19] Dattatreya, J., Rajamane, N., Sabitha, D., Ambily, P., & Nataraja, M. (2011). Flexural behaviour of reinforced geopolymer concrete beams. *Int J Civ Struct Eng*, 2(1), 138–159.
- [20] Yost, J. R., Radlińska, A., Ernst, S., Salera, M., & Martignetti, N. J. (2013). Structural behavior of alkali activated fly ash concrete. Part. Structural testing and experimental findings. *Mater Struct*, 46(3), 449–462. [CrossRef]
- [21] Kumaravel, S., & Thirugnanasambandam, S. (2013). Flexural behaviour of reinforced low calcium fly ash based geopolymer concrete beam. *Glob J Res Eng*, 13(8), 8–14.
- [22] Kumaravel, S., Thirugnanasambandam, S., & Jeyasehar, A. (2014). Flexural behavior of geopolymer concrete beams with GGBS. *IUP J Struct Eng*, 7(1), 45–54.
- [23] Yodsudjai, W. (2014). Application of fly ash-based geopolymer for structural member and repair materials. *13th Int Ceram Congr - Part F*, 92, 74–83. [CrossRef]
- [24] Madheswaran, C., Ambily, P., Rajamane, N., & Arun, G. (2014). Studies on flexural behaviour of reinforced geopolymer concrete beams with lightweight aggregates. *Int J Civ Struct Eng*, 4(3), 295–305. [CrossRef]
- [25] Hutagi, A., & Khadiranaikar, R. B. (2016). Flexural behavior of reinforced geopolymer concrete beams. *Int Conf Electr Electron Optim Tech*, ICEEOT 2016, 3463–3467. [CrossRef]
- [26] Kumar, P. U., & Kumar, B. S. (2016). Flexural behaviour of reinforced geopolymer concrete beams with GGBS and metakaoline. *Int J Civ Eng Technol*, 7(6), 260–277.
- [27] Zhang, H., Wan, K., Wu, B., & Hu, Z. (2021). Flexural behavior of reinforced geopolymer concrete beams with recycled coarse aggregates. *Adv Struct Eng*, 24(14), 3281–3298. [CrossRef]
- [28] Alex, A. G., Gebrehiwet, T., Kemal, Z., & Subramanian, R. B. (2022). Structural performance of low-calcium fly ash geopolymer reinforced concrete beam. *Iran J Sci Technol Trans Civ Eng*, 46(1) 1–12. [CrossRef]
- [29] Jeyasehar, C., Saravanan, G., & Salahuddin, M. (2013). Development of fly ash based geopolymer precast concrete elements. *Asian J Civ Eng (BHRC)*, 14(4), 605–616
- [30] Zinkaah, O. H., Araba, A., & Alhawat, M. (2021). Performance of ACI code for predicting the flexural capacity and deflection of reinforced geopolymer concrete beams. *IOP Conf Ser Mater Sci Eng*, 1090(1), 012067. [CrossRef]
- [31] Srinivasan, S., Karthik, A., & Nagan, D. S. (2014). An investigation on flexural behaviour of glass fibre reinforced geopolymer concrete beams. *Int J Eng Sci Res Technol*, 3(4), 1963–1968.
- [32] Devika, C. P., Deepthi, R. (2015). Study of flexural behavior of hybrid fiber reinforced geopolymer concrete beam. *Int J Sci Res (IJSR)*, 4(7), 130–135.
- [33] Kumar, V. S., Ganesan, N., & Indira, P. V. (2021). Shear strength of hybrid fibre-reinforced ternary blend geopolymer concrete beams under flexure. *Materials*, 14(21), 6634. [CrossRef]
- [34] Abraham, R., Raj, S., & Abraham, V. (2013). Strength and behaviour of geopolymer concrete beams. *Int J Innov Res Sci Eng Technol*, 2(1), 159–166.
- [35] Mourougane, R., Puttappa, C., Sashidhar, C., & Muthu, K. (2012). Shear behaviour of high strength GPC/TVC beams. *Proc Int Conf Adv Arch Civ Eng*, 21, 142.
- [36] Chang, E. H., Sarker, P., Lloyd, N., & Rangan, B. V. (2009). Bond behaviour of reinforced fly ash-based geopolymer concrete beams. *Concrete Solutions 09, The 24th Biennial Conf of the Concrete Inst of Australia*, pp. 1–10.

- [37] Çelik, A. İ., Özbayrak, A., Şener, A., & Acar, M. C. (2022). Effect of activators in different ratios on compressive strength of geopolymer concrete. *Can J Civ Eng*, 50(2), 69–79. [CrossRef]
- [38] Çelik, A. İ., Özbayrak, A., Şener, A., & Acar, M. C. (2022). Numerical analysis of flexural and shear behaviors of geopolymer concrete beams. *J Sustain Constr Mater Technol*, 7(2), 70–80. [CrossRef]
- [39] Shrestha, R., Baweja, D., Neupane, K., Chalmers, D., & Sleep, P. (2013). Mechanical properties of geopolymer concrete: Applicability of relationships defined by AS 3600. *Concrete Inst of Australia-Biennial Conf*, 3600(2014), 3600.
- [40] Chi, M. (2012). Effects of dosage of alkali-activated solution and curing conditions on the properties and durability of alkali-activated slag concrete. *Constr Build Mater*, 35, 240–245. [CrossRef]
- [41] Farhan, N. A., Sheikh, M. N., & Hadi, M. N. S. (2019). Investigation of engineering properties of normal and high strength fly ash based geopolymer and alkali-activated slag concrete compared to ordinary Portland cement concrete. *Constr Build Mater*, 196, 26–42. [CrossRef]
- [42] Zhang, P., Gao, Z., Wang, J., Guo, J., Hu, S., & Ling, Y. (2020). Properties of fresh and hardened fly ash/slag based geopolymer concrete: A review. *J Clean Prod*, 270, 122389. [CrossRef]
- [43] Okoye, F. N., Durgaprasad, J., & Singh, N. B. (2015). Mechanical properties of alkali activated flyash/Kaolin based geopolymer concrete. *Constr Build Mater*, 98, 685–691. [CrossRef]
- [44] Erfanimanesh, A., & Sharbatdar, M. K. (2020). Mechanical and microstructural characteristics of geopolymer paste, mortar, and concrete containing local zeolite and slag activated by sodium carbonate. *J Build Eng*, 32, 101781. [CrossRef]
- [45] Amran, M., Al-Fakih, A., Chu, S. H., Fediuk, R., Haruna, S., Azevedo, A., & Vatin, N. (2021). Long-term durability properties of geopolymer concrete: An in-depth review. *Case Stud Constr Mater*, 15, e00661. [CrossRef]
- [46] Wardhono, A., Gunasekara, C., Law, D. W., & Setunge, S. (2017). Comparison of long-term performance between alkali activated slag and fly ash geopolymer concretes. *Constr Build Mater*, 143, 272–279. [CrossRef]
- [47] Meng, Q., Wu, C., Hao, H., Li, J., Wu, P., Yang, Y., & Wang, Z. (2020). Steel fibre reinforced alkali-activated geopolymer concrete slabs subjected to natural gas explosion in buried utility tunnel. *Constr Build Mater*, 246(3), 118447. [CrossRef]
- [48] Nguyen, K. T., Ahn, N., Le, T. A., & Lee, K. (2016). Theoretical and experimental study on mechanical properties and flexural strength of fly ash-geopolymer concrete. *Constr Build Mater*, 106, 65–77. [CrossRef]
- [49] Mo, K. H., Alengaram, U. J., & Jumaat, M. Z. (2016). Structural performance of reinforced geopolymer concrete members: A review. *Constr Build Mater*, 120, 251–264. [CrossRef]
- [50] Acar, M. C., Şener, A., Özbayrak, A., & Çelik, A. İ. (2020). The effect of zeolite additive on geopolymer mortars. *J Eng Sci Des*, 8(3), 820–832. [CrossRef]
- [51] Lee, W. K. W., & Van Deventer, J. S. J. (2002). Structural reorganisation of class F fly ash in alkaline silicate solutions. *Colloids Surf A Physicochem Eng Asp*, 211(1), 49–66. [CrossRef]
- [52] ACI Committee 318. (2014). ACI 318-14: *Building Code Requirements for Structural Concrete and Commentary*.
- [53] Turkish Standarts. (2000). Requirements for design and construction of reinforced concrete structures. TS-500.
- [54] Bhushan H. Shinde, & Dr. Kshitija N. Kadam. (2015). Properties of fly ash based geopolymer mortar. *Int J Eng Res*, 4(7), 971–974. [CrossRef]
- [55] Özbayrak, A., Kucukgoncu, H., Atas, O., Aslanbay, H. H., Aslanbay, Y. G., & Altun, F. (2023). Determination of stress-strain relationship based on alkali activator ratios in geopolymer concretes and development of empirical formulations. *Structures*, 48, 2048–2061. [CrossRef]
- [56] Prachasaree, W., Limkatanyu, S., Samakrattakit, A., & Hawa, A. (2014). Development of equivalent stress block parameters for fly-ash-based geopolymer concrete. *Arab J Sci Eng*, 39, 8549–8558. [CrossRef]
- [57] Tempest, B., Gergely, J., & Skipper, A. (2016). Reinforced geopolymer cement concrete in flexure: A closer look at stress-strain performance and equivalent stress-block parameters. *PCI J*, 61(6), 30–43. [CrossRef]
- [58] Tran, T. T., Pham, T. M., & Hao, H. (2019). Rectangular stress-block parameters for fly-ash and slag based geopolymer concrete. *Structures*, 19, 143–155. [CrossRef]
- [59] Hardjito, D., & Rangan, B. V. (2005). Development and properties of low-calcium fly ash-based geopolymer concrete. *Curtin University of Technology*, pp. 1–94.
- [60] Farooq, F., Rahman, S. K. U., Akbar, A., Khushnood, R. A., Javed, M. F., Alyousef, R., alabduljabbar, H., & aslam, F. (2020). A comparative study on performance evaluation of hybrid GNPs/CNTs in conventional and self-compacting mortar. *Alex Eng J*, 59(1), 369–379. [CrossRef]
- [61] Viet Hung, T., Duy Tien, N., & Van Dong, D. (2017). Experimental study on section curvature and ductility of reinforced geopolymer concrete beams. *Sci J Transp*, 8, 3–11.
- [62] Fernández-Jiménez, A. M., Palomo, A., & López-Hombrados, C. (2006). Engineering properties of alkali-activated fly ash concrete. *ACI Mater J*, 103(2), 106–112. [CrossRef]
- [63] Liu, Y., Shi, C., Zhang, Z., Li, N., & Shi, D. (2020). Mechanical and fracture properties of ultra-high performance geopolymer concrete: Effects of steel fiber and silica fume. *Cem Concr Compos*, 112, 103665. [CrossRef]

- [64] Sofi, M., van Deventer, J. S. J., Mendis, P. A., & Lukey, G. C. (2007). Engineering properties of inorganic polymer concretes (IPCs). *Cem Concr Res*, 37(2), 251–257. [CrossRef]
- [65] Mohammed, A. A., Ahmed, H. U., & Mosavi, A. (2021). Survey of mechanical properties of geopolymer concrete: A comprehensive review and data analysis. *Materials*, 14(16), 4690. [CrossRef]
- [66] Verma, M., Dev, N., & Research, O. (2021). Geopolymer concrete: A sustainable and economic concrete via experimental analysis. <https://www.researchsquare.com/article/rs-185150/v1> [CrossRef]
- [67] Ding, Y., Dai, J. G., & Shi, C. J. (2016). Mechanical properties of alkali-activated concrete: A state-of-the-art review. *Constr Build Mater*, 127, 68–79. [CrossRef]
- [68] Cong, X., Zhou, W., & Elchalakani, M. (2020). Experimental study on the engineering properties of alkali-activated GGBFS/FA concrete and constitutive models for performance prediction. *Constr Build Mater*, 240, 117977. [CrossRef]
- [69] Xin, L., Xu, J. Y., Li, W., & Bai, E. (2014). Effect of alkali-activator types on the dynamic compressive deformation behavior of geopolymer concrete. *Mater Lett*, 124, 310–312. [CrossRef]
- [70] Ou, Z., Feng, R., Mao, T., & Li, N. (2022). Influence of mixture design parameters on the static and dynamic compressive properties of slag-based geopolymer concrete. *J Build Eng*, 53, 104564. [CrossRef]
- [71] Huda, M. N., Jumat, M. Z. Bin, & Islam, A. B. M. S. (2016). Flexural performance of reinforced oil palm shell & palm oil clinker concrete (PSCC) beam. *Constr Build Mater*, 127, 18–25. [CrossRef]
- [72] Yap, S. P., Bu, C. H., Alengaram, U. J., Mo, K. H., & Jumaat, M. Z. (2014). Flexural toughness characteristics of steel–polypropylene hybrid fibre-reinforced oil palm shell concrete. *Mater Des*, 57, 652–659. [CrossRef]
- [73] Liu, Y., Zhang, Z., Shi, C., Zhu, D., Li, N., & Deng, Y. (2020). Development of ultra-high performance geopolymer concrete (UHPC): Influence of steel fiber on mechanical properties. *Cem Concr Compos*, 112, 103670. [CrossRef]
- [74] Bhutta, A., Borges, P. H. R., Zanotti, C., Farooq, M., & Banthia, N. (2017). Flexural behavior of geopolymer composites reinforced with steel and polypropylene macro fibers. *Cem Concr Compos*, 80, 31–40. [CrossRef]
- [75] Zhang, H., Wan, K., Wu, B., & Hu, Z. (2021). Flexural behavior of reinforced geopolymer concrete beams with recycled coarse aggregates. *Adv Struct Eng*, 24(14), 3281–3298. [CrossRef]
- [76] Özbayrak, A., Kucukgoncu, H., Aslanbay, H. H., Aslanbay, Y. G., & Atas, O. (2023). Comprehensive experimental analysis of the effects of elevated temperatures in geopolymer concretes with variable alkali activator ratios. *J Build Eng*, 68, 106108. [CrossRef]
- [77] Aslanbay, Y. G., Aslanbay, H. H., Özbayrak, A., Kucukgoncu, H., & Atas, O. (2024). Comprehensive analysis of experimental and numerical results of bond strength and mechanical properties of fly ash based GPC and OPC concrete. *Constr Build Mater*, 416, 135175. [CrossRef]
- [78] Cecen, F., Özbayrak, A., & Aktaş, B. (2023). Experimental modal analysis of fly ash-based geopolymer concrete specimens via modal circles, mode indication functions, and mode shape animations. *Cem Concr Compos*, 137, 104951. [CrossRef]